

# TIP ANGLE EFFECT ON BUCKLING AND DEFORMATION OF LAMINATED COMPOSITE ANGLEGRID PLATES

A. Ehsani<sup>1</sup> and H. Dalir<sup>2</sup>

<sup>1,2</sup> Department of Mechanical and Energy Engineering, Purdue School of Engineering and Technology, Indianapolis, United States

Email: ehsani@iupui.edu

Email: hdalir@iupui.edu

**Keywords:** Laminated grid, Anglegrid, Buckling, Deformation

## Abstract

Grid structures are widely used in many engineering fields. Typically, a single grid plate is employed as an orthotropic layer to strengthen plates and shells or as an independent structural element. In contrast with conventional grids, laminated grid plates are constituted from several grid layers with various orientations. Therefore, the grid layers with different orientations can be utilized to enhance stiffness and coupling effects of a weight sensitive structure. In the present study, to investigate the efficiency of the laminated anglegrids, the deformation and buckling responses of a conventional and several laminated anglegrid plates are evaluated. The first-order shear deformation plate theory along with Ritz method is employed to achieve the buckling load and maximum deflection of the plates. The effectiveness of modifying the tip angle of anglegrid layers on mechanical behaviors of the conventional and laminated grids is also studied. The analytical results of buckling load are compared and validated by finite element method. The results indicate that thoughtful selection of stacking sequences of the laminated grids and appropriate tip angle considerably improves the behavior of the laminated grids in comparison with conventional grids.

## 1. Introduction

The grid structures are designed to tolerate loads in specific directions. This preference can decrease the weight of structures[1]. Due to exceptional properties of the reinforced composite materials, low weight, directional and tailorable properties, they are widely used in weight sensitive structures such as grids. There are many known grid patterns in industries, namely, isogrid, orthogrid, and anglegrid and they can be utilized in different applications. Thus far, most investigations are concentrated on mechanical behavior prediction, fabrication, and optimization of single layer grid structures, which will be called conventional grids. Gürdal and Gendron [2] evaluated the structural efficiency of geodesically stiffened shells with various stiffener arrangements under compression, torsion and combined loads. Jaunky et al. [3] proposed an improved smeared stiffener theory for stiffened panels including skinstiffener interaction effects. They showed; the result of the new method is more accurate than common smeared stiffener approach. Bedair [4] studied the effects of stiffener position on the stability of stiffened plates subjected to compression and in-plane bending. He presented a strategy to optimize the location of the stiffeners. Prusty [5] applied the FEM to analyze free vibration and buckling of laminated stiffened panels using arbitrarily oriented stiffener formulation. Shi et al. [6] investigated the global and local buckling of grid stiffened carbon fiber thin shell structures subjected to external pressure. They used the hybrid genetic algorithm method to specify the optimal design of the structures to reach maximum buckling load. Ren et al. [7] compared the buckling response of advanced grid stiffened structures using equivalent stiffness, finite element, and hybrid models.

Ehsani and Rezaeepazhand [8] presented a new class of grid structures which are known as “laminated grid structures”. They investigated lamination effects on stiffness and mechanical behavior of grid structures. Ehsani et al. [9, 10] studied the influence of the stacking sequence and pattern composition on buckling load of laminated composite grid plates and also conducted studies on the buckling load and natural vibration of laminated orthogrid plates. Their results showed that, there are proper stacking sequences, which considerably improves the mechanical behaviors of the grid structures.

Similar to laminated structures, in a laminated grid, each single grid layer is assumed as a lamina. Hence, a laminated grid is composed of various single grid layers (conventional grids) with different stacking sequences (orientations). Fig.1 illustrates two types of anglegrid structures. Fig.1a shows a laminated anglegrid plate which is composed of three anglegrid layers, with  $(0^\circ/90^\circ/0^\circ)$  stacking sequence. Fig.1b illustrates a conventional anglegrid plate.

Several advantages can be named for employing laminated grid structures instead of the conventional grids such as ability to use different fibers, orientations, thicknesses, and patterns (isogrid, anglegrid, etc.) in each grid layer and accessibility to wide range of coupling effects of laminated grid structures.

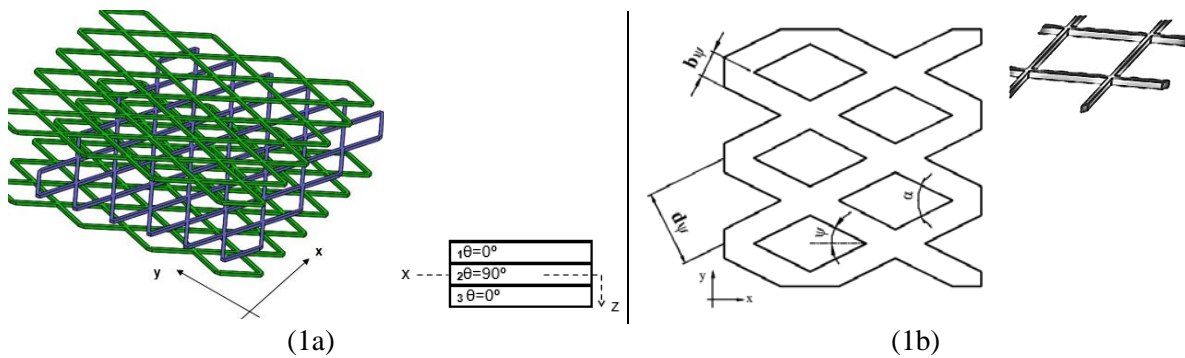


**Figure 1.** A laminated anglegrid plate, with three anglegrid layers and  $(0^\circ/90^\circ/0^\circ)$  lay-up (1a), a conventional anglegrid plate with tip angle  $\alpha$  (1b)

Although, the conventional composite grid structures have been extensively studied, there are limited attention to the laminated anglegrid structures and their tip angle effect on the structural performances. In the present study, the axial buckling load and maximum lateral deformation of laminated and conventional anglegrid plates are obtained employing Mindlin theory. The effectiveness of using different tip angles along with various orientation of each grid layer is also evaluated. To ensure the accuracy of results, some selected results are compared and validated with finite element results achieved using ABAQUS software.

## 2. Problem Description

### 2.1. Laminated Grid Configuration

A laminated grid consists of several grid layers which the pattern, thickness and orientation of each layer can be varied [10]. In the current work, the laminated grids are composed of several composite anglegrid layers. Three cases of grid structures have been considered in this study. In all cases ribs' width,  $b_\psi$ , is identical (see Fig.1) and the thickness of the structures are defined to have identical weight in all cases. Ribs' spacing distance,  $d_\psi$ , is changed based on the tip angle of a grid layer. The plates have square geometry with side  $a$ , and symmetrical arrangement respect to mid-plane. The structures are considered to have simply support boundary condition along all edges.

The first case is a single layer anglegrid or conventional anglegrid. The second case is a sub-laminate grid structure with  $(\pm\theta)_s$  configuration and four layers. To investigate the effect of increasing the layers, the third one is considered to be a sub-laminate grid structure with  $(\pm\theta)_{5s}$  configuration and twenty

layers (see Table 1). It is assumed that the grid layers are without any initial imperfection or defect and are perfectly bonded to each other. Table 1 presents the characteristics of the defined cases. In a laminated grid, each grid layer may have any arbitrary orientation ( $\theta$ ). Fig. 4 illustrates a special anglegrid and a general anglegrid plate, which is rotated  $\theta$  degree with respect to  $X$  direction.

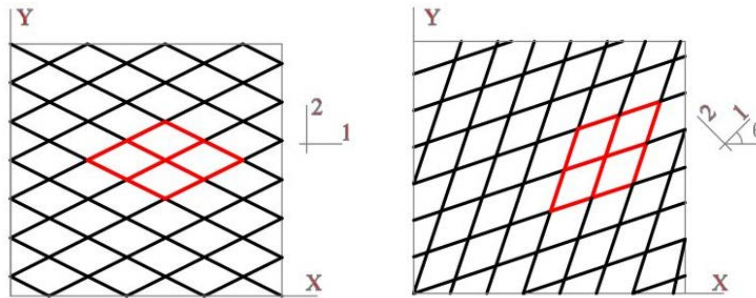


**Figure 2.** A specially anglegrid ( $\theta=0$ ) (left). A general anglegrid that is rotated  $\theta$  degree with respect to  $x$  direction (right).

The grid layers are made of carbon/epoxy material with the following elastic and strength properties:  $E_1=48 \text{ GPa}$ ,  $E_2=15.3 \text{ GPa}$ ,  $G_{12}=5.1 \text{ GPa}$ ,  $\nu_{12}=0.315$ , and density= $2112 \text{ kg/m}$  [11] where  $E_1$ ,  $E_2$ , and  $G_{12}$  are the longitudinal, transvers elastic and shear modules of the applied material, respectively.

**Table 1.** The characteristics of the considered cases

Case #	Type of grid structure	Lay-up name	Stacking sequence	Number of layers (N)
1	Laminated anglegrid	Sub-laminate	$(\pm\theta^0)_{5s}$	20
2	Laminated anglegrid	Sub-laminate	$(\pm\theta^0)_s$	4
3	Conventional anglegrid	Anglegrid	$(\theta^0)$	1

## 2.2. Constitutive Equations

The first-order shear deformation plate theory (FSDT) along with Ritz method is considered to obtain the buckling load and maximum deflection of the plates. Based on FSDT, the displacement field for a plate can be expressed as:

$$u=u_0(x, y, t)+z\varphi_x(x, y, t) \quad (1a)$$

$$v=v_0(x, y, t)+z\varphi_y(x, y, t) \quad (1b)$$

$$w=w(x, y, t) \quad (1c)$$

Where  $u$ ,  $v$  and  $w$  are the displacement components in  $x$ ,  $y$  and  $z$  directions and  $\varphi_x$  and  $\varphi_y$  are the bending slope along  $y$  and  $x$  axis, respectively.

The grid layer has directional properties. Therefore, the stress displacement relations for a special anglegrid Mindlin plate can be written as [12]:

$$\begin{Bmatrix} \sigma_{xx} \\ \sigma_{yy} \\ \sigma_{xy} \\ \sigma_{yz} \\ \sigma_{xz} \end{Bmatrix} = \begin{bmatrix} \bar{Q}_{11} & \bar{Q}_{12} & \bar{Q}_{16} & 0 & 0 \\ \bar{Q}_{12} & \bar{Q}_{22} & \bar{Q}_{26} & 0 & 0 \\ \bar{Q}_{16} & \bar{Q}_{26} & \bar{Q}_{66} & 0 & 0 \\ 0 & 0 & 0 & \bar{Q}_{44} & \bar{Q}_{45} \\ 0 & 0 & 0 & \bar{Q}_{45} & \bar{Q}_{55} \end{bmatrix} \begin{Bmatrix} u_{0,x} \\ v_{0,y} \\ u_{0,y}+v_{0,x} \\ \varphi_y+w_{,y} \\ \varphi_x+w_{,x} \end{Bmatrix} + z \begin{Bmatrix} \varphi_{x,x} \\ \varphi_{y,y} \\ \varphi_{x,y}+\varphi_{y,x} \\ 0 \\ 0 \end{Bmatrix} \quad (2)$$

$[\bar{Q}]$  is the transferred reduced stiffness matrix and can be obtained as below:

$$[\bar{Q}] = [T]^{-1} [Q] [T]^T \quad (3)$$

$[T]$  is the transformation matrix [13] which depends on the grid layer orientation,  $\theta$ . For an anglegrid layer,  $[Q]$  is calculated according to the method presented by Nemeth [14]. Hence, the reduced stiffness elements for the specially anglegrid plate can be given as the following forms:

$$\begin{aligned} Q_{11} &= \frac{2Eb\psi}{d\psi} \cos^4 \psi + \frac{2G_{XY}b\psi}{d\psi} \cos^2 \psi \sin^2 \psi \\ Q_{12} = Q_{21} &= \left( \frac{Eb\psi}{d\psi} - \frac{G_{XY}b\psi}{d\psi} \right) \cos^2 \psi \sin^2 \psi \\ Q_{22} &= \frac{2Eb\psi}{d\psi} \sin^4 \psi + \frac{2G_{XY}b\psi}{d\psi} \cos^2 \psi \sin^2 \psi \\ Q_{66} &= \frac{2Eb\psi}{d\psi} \cos^2 \psi \sin^2 \psi + \frac{2G_{XY}b\psi}{d\psi} (\cos^2 \psi - \sin^2 \psi) \\ Q_{44} &= 2G_{YZ} \left( \frac{b\psi}{d\psi} \sin^2 \psi \right) \\ Q_{55} &= 2G_{XZ} \left( \frac{b\psi}{d\psi} \cos^2 \psi \right) \end{aligned} \quad (4)$$

Where  $\psi$ ,  $b_\psi$ , and  $d_\psi$  are the geometry parameters, which are illustrated in Fig.1.  $E$ ,  $G_{XY}$ ,  $G_{YZ}$ , and  $G_{XZ}$  are the longitudinal elastic and shear modules of applied composite material and it is assumed that the material properties of ribs are identical. The force and moment resultants  $N$ ,  $M$ , and  $Q$  are defined as:

$$(N_x, N_y, N_{xy}, M_x, M_y, M_{xy}, Q_x, Q_y) = \int_{-\frac{H}{2}}^{\frac{H}{2}} (\sigma_x, \sigma_y, \sigma_{xy}, z\sigma_x, z\sigma_y, z\sigma_{xy}, \tau_{xz}, \tau_{yz}) dz \quad (5)$$

Substituting Eq. (2) into Eq. (5), the resultant forces and moments for a symmetric laminated grid are achieved.

$$\begin{Bmatrix} \tilde{N} \\ \tilde{M} \end{Bmatrix} = \begin{bmatrix} [A] & 0 \\ 0 & [D] \end{bmatrix} \begin{Bmatrix} \tilde{\varepsilon} \\ \tilde{\kappa} \end{Bmatrix} \quad (6a)$$

$$\begin{Bmatrix} Q_x \\ Q_y \end{Bmatrix} = K_s \begin{bmatrix} A_{44} & 0 \\ 0 & A_{55} \end{bmatrix} \begin{Bmatrix} \gamma'_{yz} \\ \gamma'_{xz} \end{Bmatrix} \quad (6b)$$

Where  $\varepsilon$  and  $\kappa$  are the strains and curvatures of the mid-plane, respectively,  $K_s$  is the shear correction factor and  $[A]$  and  $[D]$  are the extensional and bending stiffness matrices of the laminated grid [13]:

$$A_{ij} = \sum_{k=1}^N (\bar{Q}_{ij})_k (z_k - z_{k-1}) \quad i, j = 1, 2, 4, 5, 6 \quad (7a)$$

$$D_{ij} = \sum_{k=1}^N (\bar{Q}_{ij})_k \left[ \frac{1}{3} (z_k^3 - z_{k-1}^3) \right] \quad i, j = 1, 2, 6 \quad (7b)$$

Where,  $k$  is the layer number in the laminate,  $z_k$  is distance of  $k$  layer from the middle surface, and  $N$  is the number of the grid layers.

For a simply supported plate, the functions that satisfy the geometrical boundary conditions for  $w$ ,  $\varphi_x$  and  $\varphi_y$  in Eq. 1 can be presented as the following series [15]:

$$w(x,y) = \sum_{m=1}^M \sum_{n=1}^N W_{mn} \sin\left(\frac{m\pi}{a}x\right) \sin\left(\frac{n\pi}{b}y\right) \quad (8a)$$

$$\varphi_x(x,y) = \sum_{m=1}^M \sum_{n=1}^N B_{mn} \cos\left(\frac{m\pi}{a}x\right) \sin\left(\frac{n\pi}{b}y\right) \quad (8b)$$

$$\varphi_y(x,y) = \sum_{m=1}^M \sum_{n=1}^N C_{mn} \sin\left(\frac{m\pi}{a}x\right) \cos\left(\frac{n\pi}{b}y\right) \quad (8c)$$

Where the  $W_{mn}$ ,  $B_{mn}$  and  $C_{mn}$  are the constants.

The Ritz method has been employed to achieve the buckling load and natural frequencies of the plates. Accordingly, the total potential energy of the plate is calculated and can be expressed as:

$$\pi = U - V \quad (9)$$

Where  $U$  and  $V$  are the strain energy and loss in the potential energy, respectively. For the laminated Mindlin plate,  $U$  and  $V$  are given by Reddy [16] and Dawe [17] respectively. Implementing a minimization procedure of the total potential energy with respect to  $W_{mn}$ ,  $B_{mn}$ , and  $C_{mn}$  constants in absence of the lateral force, the following eigenvalue equation is achieved:

$$(K - \lambda K_G) \tilde{d} = 0 \quad (10)$$

Where  $K$  is the elastic stiffness matrix,  $K_G$  is the geometric stiffness matrix and  $\tilde{d}$  is the coefficient vector, which has the following form:

$$\tilde{d} = \begin{Bmatrix} W_{mn} \\ B_{mn} \\ C_{mn} \end{Bmatrix} \quad (11)$$

Obtaining the variable  $\lambda$  from Eq. 11, the buckling load will be calculated. Minimizing total energy from Eq. 9 with respect to the unknown  $W_{mn}$ ,  $B_{mn}$ , and  $C_{mn}$  constants in absence of buckling loads, several linear and simultaneous equations will be produced. Applying the mid-plane coordinate of the plate, the  $w$ ,  $\varphi_x$  and  $\varphi_y$  will be achieved.

### 3. Results and Discussion

#### 3.1. Lateral Deformation

Figs. 3 to 5, show maximum deformation for the presented cases subjected to an equal arbitrary load. To evaluate the effects of layer orientation,  $\theta$ , this parameter has been varied from  $0$  to  $90$  degrees. Moreover, to study the effect of tip angle,  $\alpha$ , on the maximum lateral deformation of the plate, the tip angle is considered to change from  $10$  to  $90$  degrees and each corresponding graph is presented in the figures.

As can be seen in the figures, the tip angle can considerably affect the deflection of the plate. According to Figs. 3 and 4, the plate with right tip angle,  $\alpha=90^\circ$ , has the maximum lateral deformation among others at  $\theta=45^\circ$  and minimum deformation at  $\theta=0^\circ$ . Therefore, as the  $\theta=0^\circ$  means the plate is a conventional anglegrid plate, using laminated grid will not be a suitable choice if the tip angle be equal to  $90$ . It should be noticed if this type not applied in proper direction, the maximum deformation of the plate is dramatically increased. However, for anglegrid plates, which they tip angle is lower than  $90^\circ$ , using laminated grid significantly decreases the maximum deformation of the plates and utilizing laminated

grid for these cases will be a rational choice. As can be seen in Figs. 3 and 4, increasing the number of layers the maximum deformation of the plates is considerably decreased.

As the Fig. 5 illustrates, the plate with right tip angle has the minimum mid-plane deformation among other types of anglegrids. Consequently, employing a right angle grid will be appropriate case among the others. As can be seen in this figure, the shape of graphs is changed when the tip angle of the structure decreases.

To evaluate the results, using Abaqus software the anglegrid plate with  $\alpha=10^\circ$  are modeled in several orientation angles,  $\theta$ , and their maximum deformation are presented for corresponding analytical results in Fig. 5. As can be seen, analytical and finite element results are in good agreement with each other.

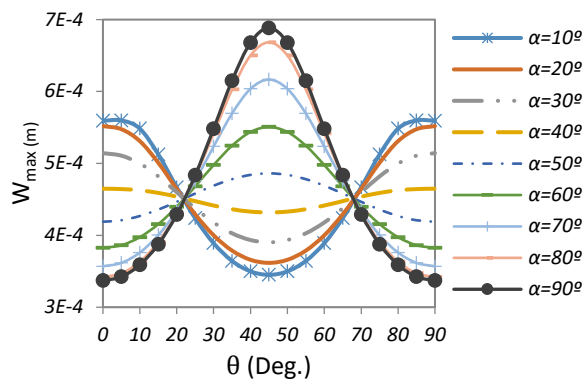


**Figure 3.** Maximum deformation of sub-laminate anglegrid plate (3<sup>rd</sup> case) for different layers orientation and various tip angles

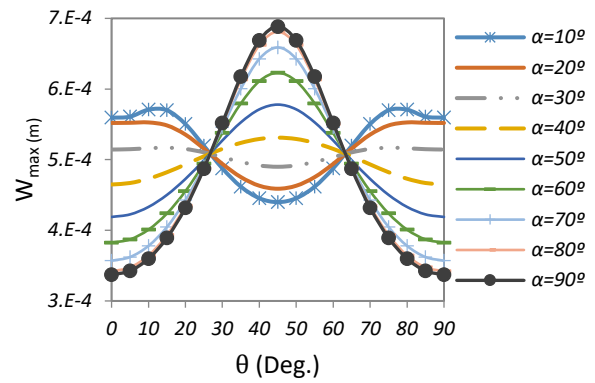


**Figure 4.** Maximum deformation of sub-laminate anglegrid plate (2<sup>nd</sup> case) for different layers orientation and various tip angles

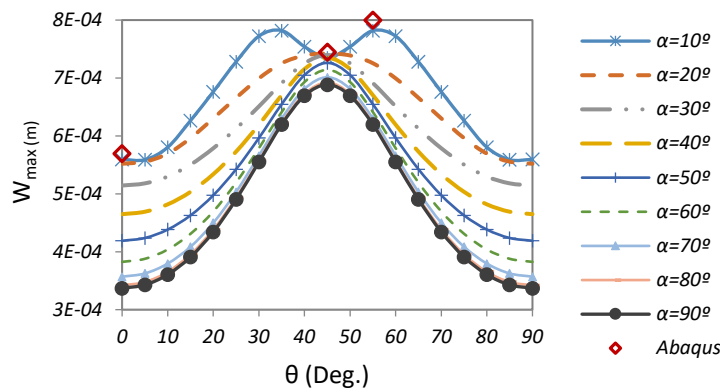


**Figure 5.** Maximum deformation of conventional anglegrid plate (1<sup>st</sup> case) for different orientation and various tip angles

### 3.2. Buckling Load

Figs. 6 to 8 depict critical axial buckling load for the presented cases in Table 1. As can be seen, in all cases the plates with right tip angle,  $\alpha=90^\circ$ , has the maximum critical buckling load at  $\theta=0^\circ$ . In the other types, the plate behavior is completely related to the tip angle of the layers. For instance, in the case  $\alpha=10^\circ$  the maximum buckling load is happened at  $\theta=45^\circ$ . Considering the following figures, it can be seen, increasing the number of layers has the significant effect on critical buckling load of the plates. For example, the buckling load of sub-laminate grid plate with  $(\pm 45)_{5s}$  configuration is about 28% more than conventional anglegrid plate at same orientation. However, the critical buckling loads for each plate will converge to an ultimate value and will not considerably affected by increasing the number of layers.

Similar to the previous session, to ensure about the analytical results, the anglegrid plate with  $\alpha=10^\circ$  are modeled in several orientation angles and their critical buckling load are obtained. According to Fig. 8, analytical and finite element results are in good agreement with each other.

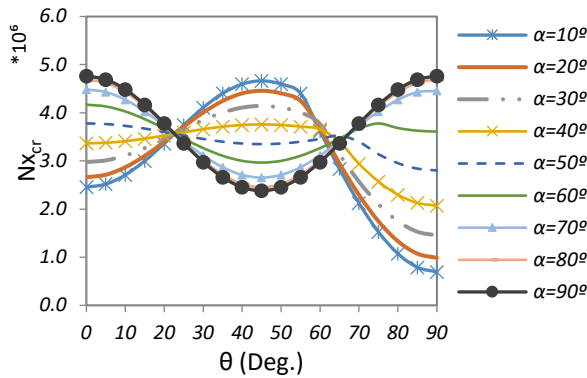


**Figure 6.** Maximum critical buckling load of sub-laminate anglegrid plate  $(\pm\theta)_s$  for different layers orientation and various tip angles

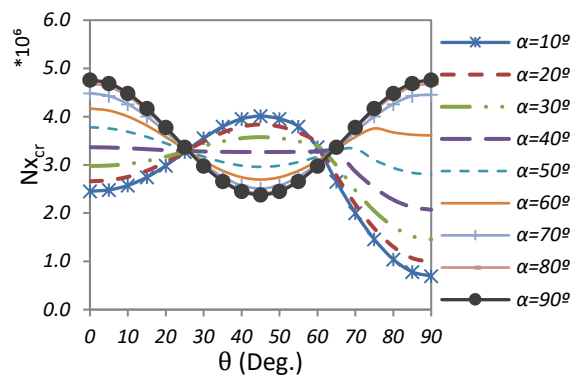


**Figure 7.** Maximum critical buckling load of sub-laminate anglegrid plate  $(\pm\theta)_s$  for different layers orientation and various tip angles

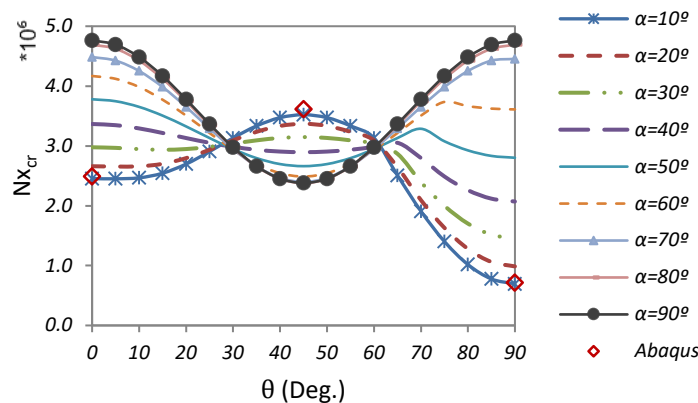


**Figure 8.** Maximum critical buckling load of conventional anglegrid plate (1<sup>st</sup> case) for different orientation and various tip angles

### 3. Conclusions

In this study, the critical buckling load and maximum lateral deformation of laminated and conventional anglegrids with identical weight are compared. To investigate the influence of number of grid layers on mechanical behaviors of a laminated grid structure, various laminated grids with different number of layers are considered. The effectiveness of modifying the tip angle of anglegrid layers on mechanical behaviors of the conventional and laminated grids is also studied. The results indicate that thoughtful selection of stacking sequences of the laminated grids and appropriate tip angle considerably improves the behavior of the laminated and conventional anglegrid structures.

The results show the grid orientation is the effective parameter in mechanical responses of the grid structures. In addition, the mechanical responses are proportional to number of grid layers of laminated grids.

### References

1. Huybrechts, S. and S.W. Tsai, *Analysis and behavior of grid structures*. Composites Science and Technology, 1996. **56**: p. 1001-1015.
2. Gürdal, Z. and G. Gendron, *Optimal design of geodesically stiffened composite cylindrical shells*. Composites Engineering, 1993. **3**: p. 1131-1147.

3. Jaunky, N., N.F. Knight Jr, and D.R. Ambur, *Formulation of an improved smeared stiffener theory for buckling analysis of grid-stiffened composite panels*. Composites Part B: Engineering, 1996. **27**(5): p. 519-526.
4. Bedair, O.K., *Influence of stiffener location on the stability of stiffened plates under compression and in-plane bending*. International Journal of Mechanical Sciences, 1997. **39**(1): p. 33-49.
5. Prusty, B.G., *Free vibration and buckling response of hat-stiffened composite panels under general loading*. International Journal of Mechanical Sciences, 2008. **50**(8): p. 1326-1333.
6. Shi, S., et al., *Buckling resistance of grid-stiffened carbon-fiber thin-shell structures*. Composites Part B: Engineering, 2013. **45**: p. 888-896.
7. Ren, M., et al., *Numerical investigation into the buckling behavior of advanced grid stiffened composite cylindrical shell*. Journal of Reinforced Plastics and Composites, 2014. **33**(16): p. 1508-1519.
8. Ehsani, A. and J. Rezaeepazhand, *Comparison of Stiffness and Failure Behavior of the Laminated Grid and Orthogrid Plates*. 2017.
9. Ehsani, A. and J. Rezaeepazhand, *Stacking sequence optimization of laminated composite grid plates for maximum buckling load using genetic algorithm*. International Journal of Mechanical Sciences, 2016. **119**: p. 97-106.
10. Ehsani, A. and J. Rezaeepazhand, *Vibration and stability of laminated composite orthogrid plates*. Journal of Reinforced Plastics and Composites, 2016. **35**: p. 1051-1061.
11. Naik, N.K., Y. Chandra Sekher, and S. Meduri, *Damage in woven-fabric composites subjected to low-velocity impact*. Composites Science and Technology, 2000. **60**: p. 731-744.
12. Yang, et al., *Buckling and bending behaviour of initially stressed specially orthotropic thick plates*. International journal of mechanical sciences, 1987. **29**(12): p. 779-791.
13. Kollar, L.P. and G.S. Springer, *Mechanics of Composite Structures*. 1 ed. 2003: Cambridge University Press.
14. Nemeth, M.P., *A Treatise on Equivalent-Plate Stiffnesses for Stiffened Laminated-Composite Plates and Plate-Like Lattices*, 2011, NASA TP 2011-216882
15. Wang, C.M., et al., *Buckling of rectangular mindlin plates with internal line supports*. International Journal of Solids and Structures, 1993. **30**(1): p. 1-17.
16. Reddy, J.N., *A penalty plate-bending element for the analysis of laminated anisotropic composite plates*. International Journal for Numerical Methods in Engineering, 1980. **15**(8): p. 1187-1206.
17. Dawe, D.J. and T.J. Craig, *The vibration and stability of symmetrically-laminated composite rectangular plates subjected to in-plane stresses*. Composite Structures, 1986. **5**(4): p. 281-307.
18. Liew, K.M., *Solving the Vibration of Thick Symmetric Laminates by Reissner/Mindlin Plate Theory and the p-Ritz Method*. Journal of Sound and Vibration, 1996. **198**(3): p. 343-360.